

# The application of dual-energy CT within the U.K. proton beam therapy service

Matthew Clarke

9<sup>th</sup> November 2023

# Introduction

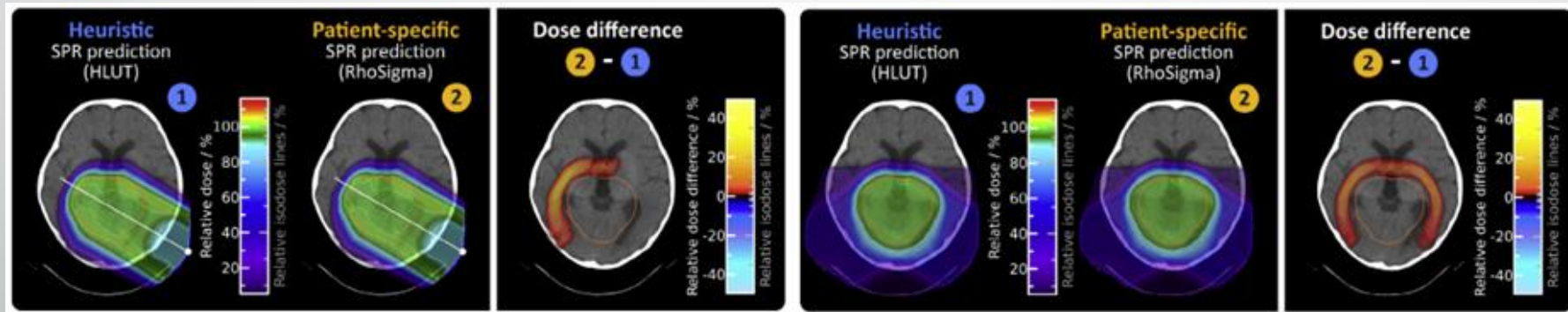
- The accurate prediction of proton stopping power ratio (SPR) is key to the effectiveness of proton beam therapy (PBT).
- The current standard method for CT calibration in PBT is to use the stoichiometric method first proposed by Schneider et al. (1996).
  - The CT scanner is parameterized in terms of its response to different elements in a compound and then transferring this elemental response into a proposed response to biological tissues of known composition.



The result is a biologically optimised HU-SPR calibration curve.

# Dual-energy CT in PBT

- Scanning at different energies illustrates differing contributions of the photoelectric effect, coherent and incoherent scattering. This improves the derivation of attenuation information for tissues.
- The potential for using DECT in treatment planning goes back to the 1970s (Goitein, 1977) but clinical applications did not appear until much later.



Wohlfahrt et al. (2017)

# Aims and objectives

Aim 1: To demonstrate that a DECT calibration can be practically implemented using the existing CT scanner and TPS.

Aim 2: To experimentally validate the DECT calibration methodology and compare to the existing solution in biological tissues.

Aim 3: To investigate the sensitivity of the DECT calibration to variables and uncertainties throughout the calibration and implementation process.

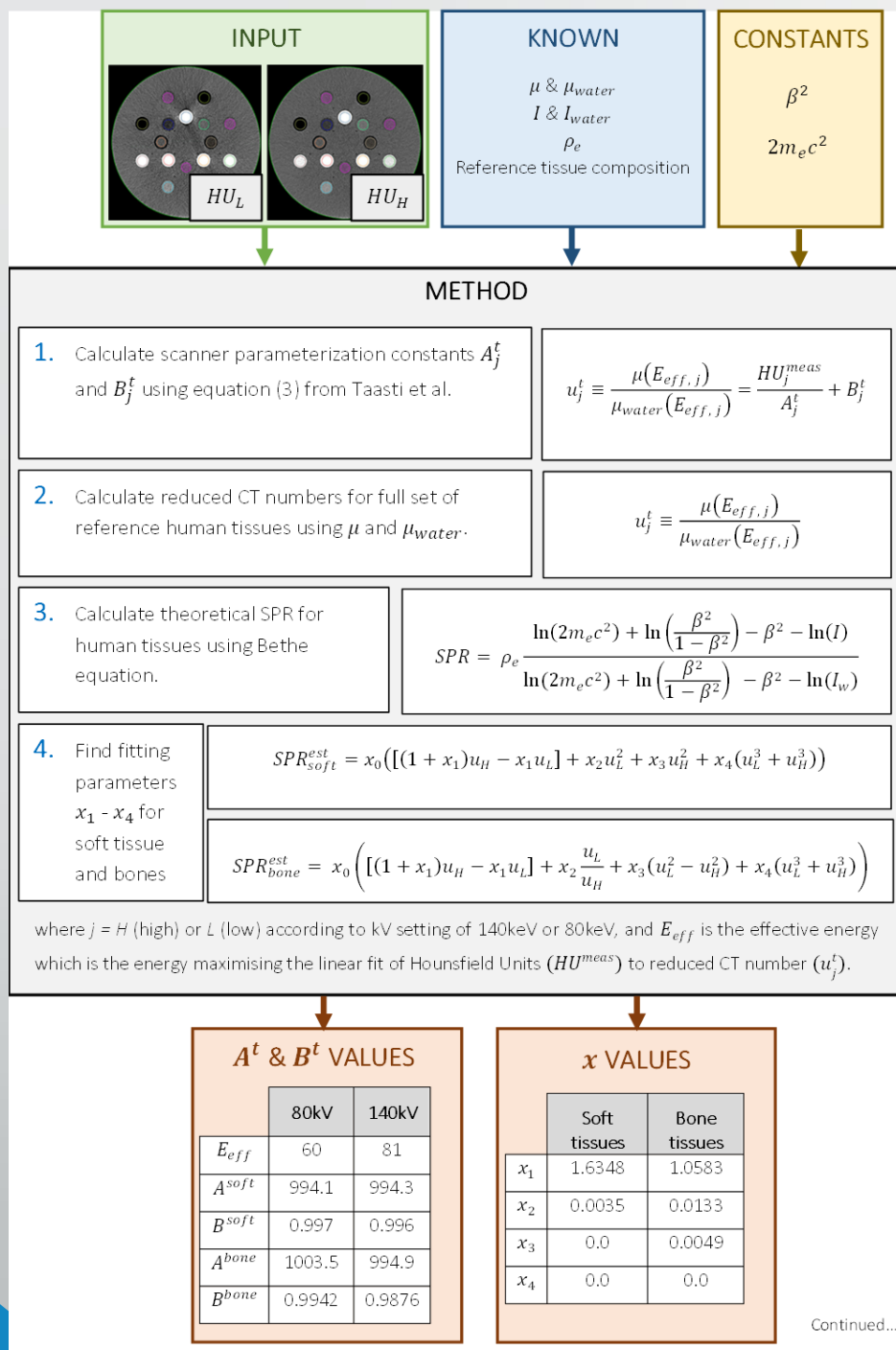
# WP<sub>1</sub>: Implementation of an empirical DECT calibration methodology for PBT treatment planning

- DECT is not currently in use for PBT planning in the U.K. This work sought to implement an empirical method first proposed by Taasti et al. (2016) and evaluate its suitability for clinical use.
  - Siemens SOMATOM Confidence scanner (dual-spiral technology) at 80 kVp and 140 kVp.
  - SPR maps generated directly using python code.
  - SPR maps imported into Eclipse TPS (v16.1).

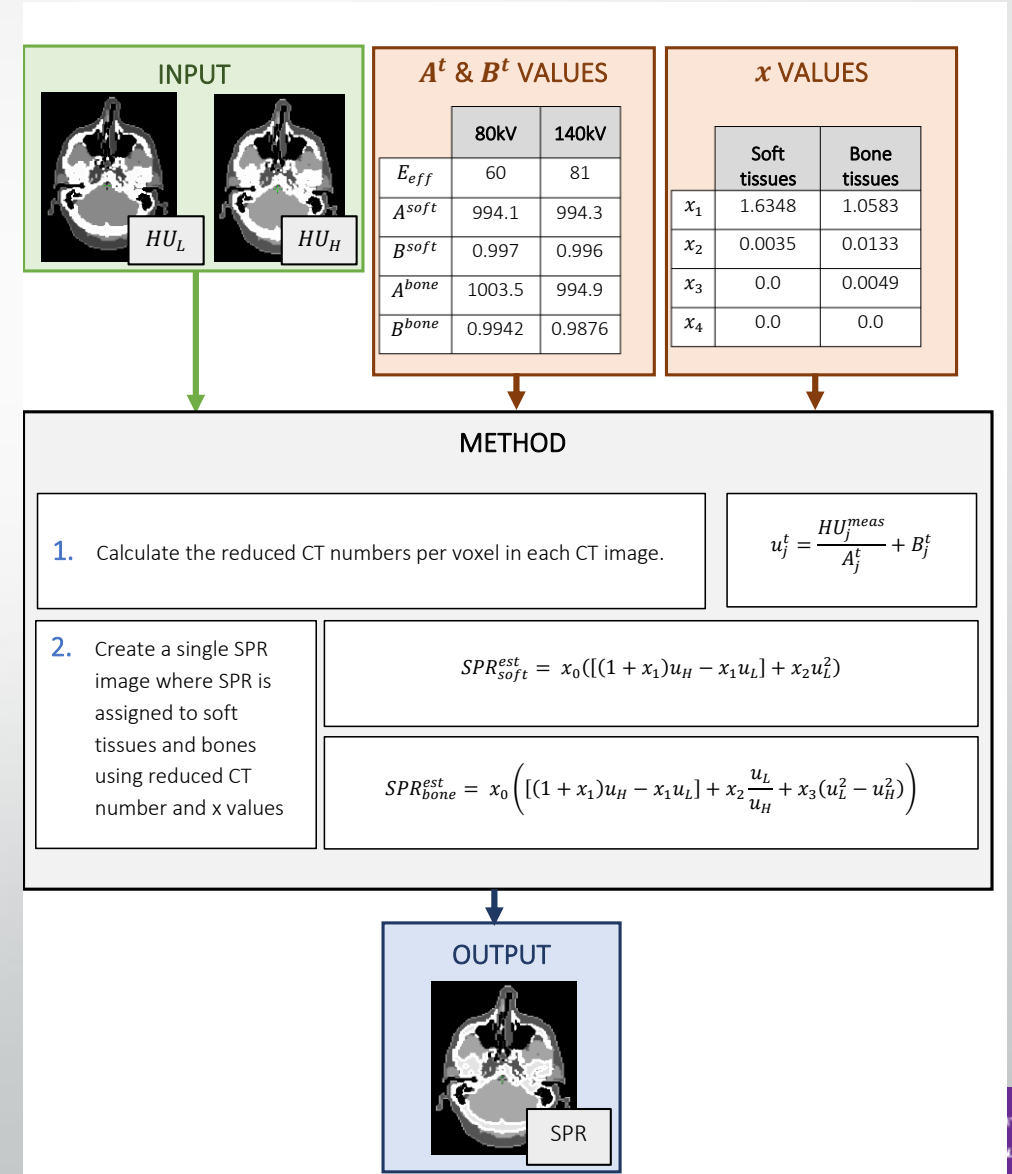


DECT methods reduced the RMSE in SPR compared to theoretical SPR for reference human tissues when compared to existing SECT techniques.

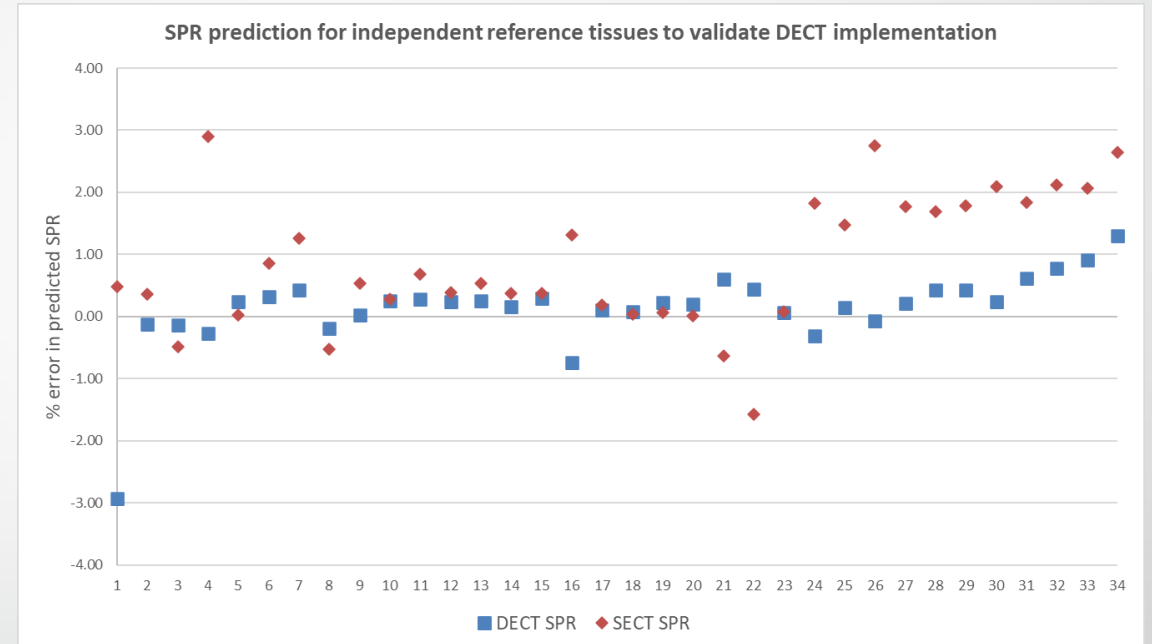
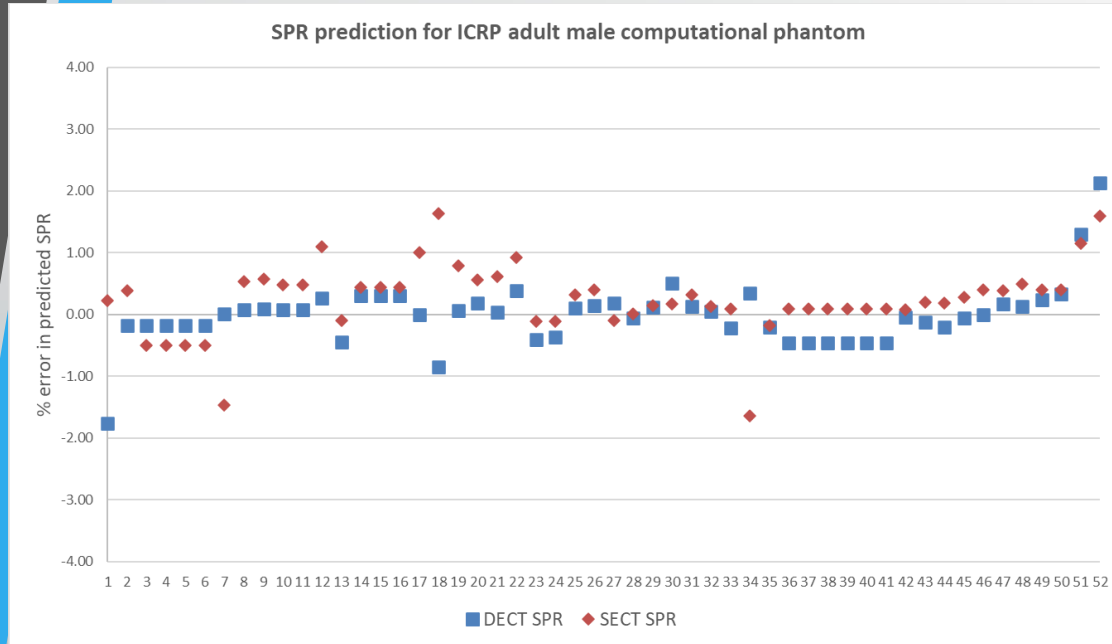
# WP1: Methods



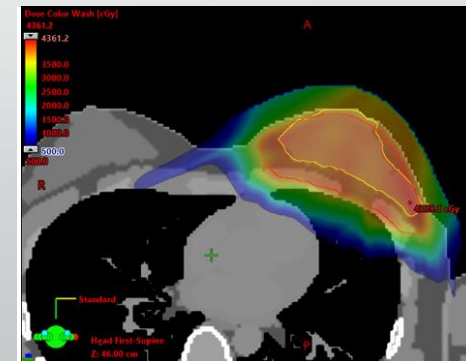
Continued...



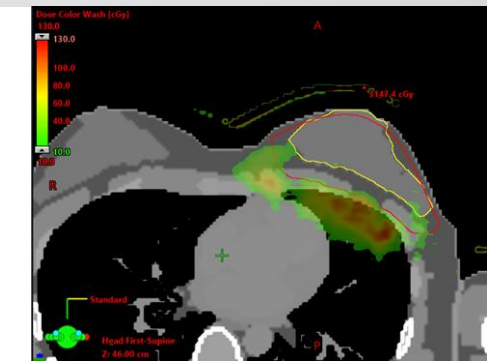
# WP1: Results



	ICRP tissues (ICRP, 2009)		Validation tissues (ICRU, 1989; White et al., 1987)	
	DECT SPR	SECT SPR	DECT SPR	SECT SPR
RMS error % (all tissues)	0.51	0.62	0.66	1.37
RMS error % (bone tissues)	0.63	0.49	0.61	2.04
RMS error % (soft tissues)	0.40	0.70	0.68	0.88
RMS error % (soft tissues excluding lung)	0.26	0.71	0.31	0.91



(a) Sample treatment plan using SECT



(b) Dose difference resulting from evaluation using DECT (SECT dose – DECT dose)

# WP<sub>1</sub>: Conclusions

- Empirical method successfully implemented using clinical systems and commercial TPS.
- Appropriate method for acquiring scans and code for applying calibration has been generated.
- This work is an effective proof of concept that DECT for PBT planning is achievable.



## WP2: Experimental validation of DECT implementation using biological samples

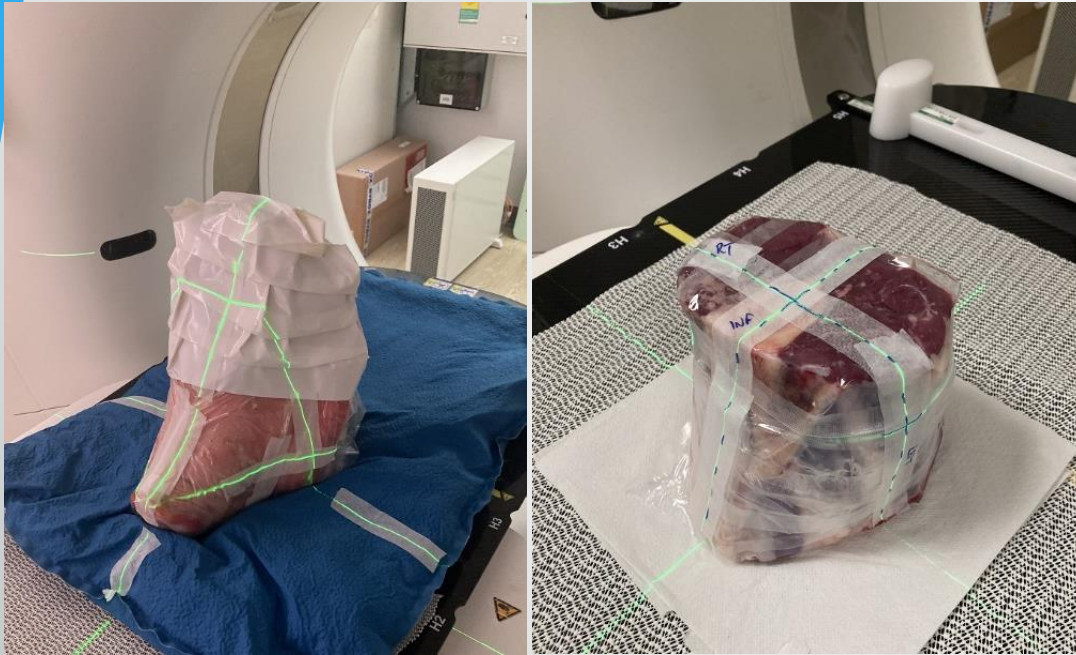
- The HU-SPR relationship is biologically optimised (using both SECT and DECT) meaning that traditional phantom-based validation of the CT calibration is not possible.
- A pig's head and a section of cow shin was used to validate the prediction of SPR using DECT against measurement using a multi-layer ionisation chamber. The accuracy of SPR prediction was compared to the current SECT method.



DECT was more accurate at predicting SPR than SECT when considering the RMSE of both soft tissues and bones together.

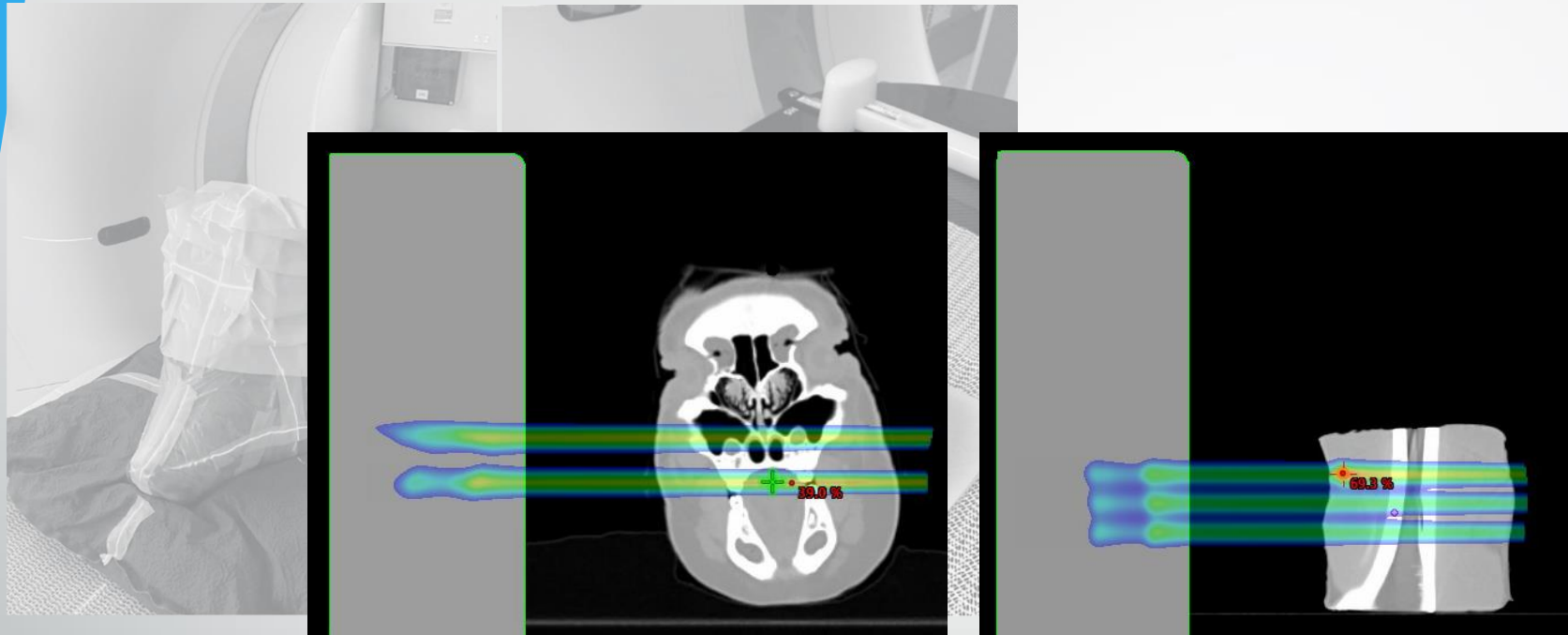
DECT did not show an improvement over SECT for all tissue types in predicting SPR compared to measurement.

# WP2: Methods



**Scan (120 kVp & 80/140 kVp)**

# WP2: Methods



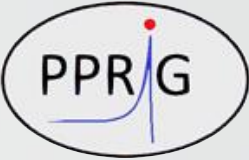
Plan (SECT & DECT)

# WP2: Methods

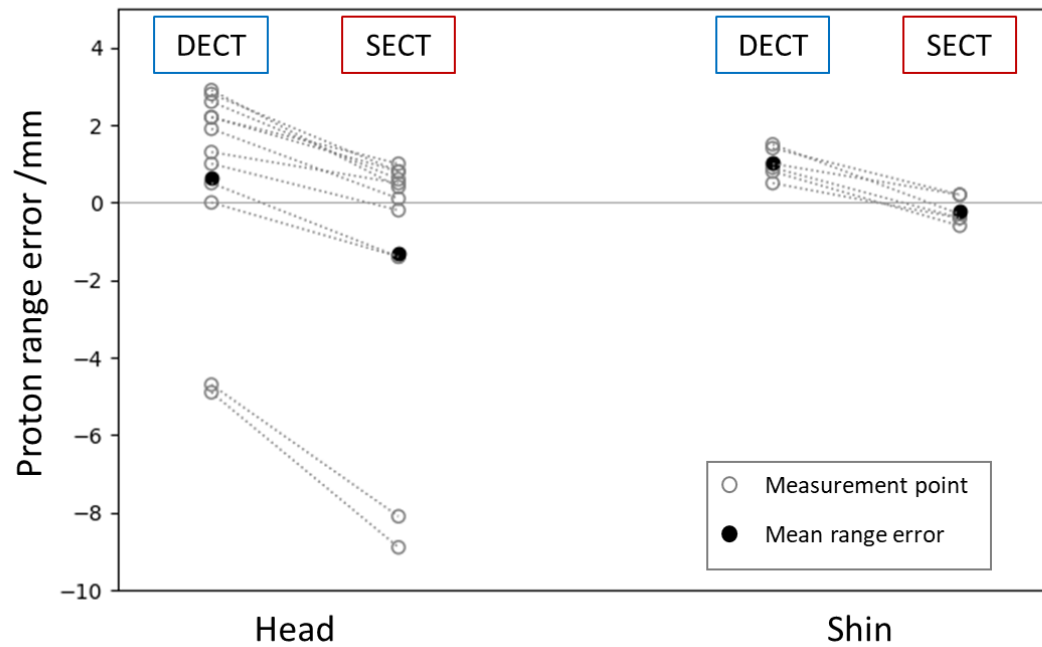


**Measure** (residual range with MLIC)

# WP2: Results



Proton predicted range – measured range for animal samples



Predicted range (R80) – measured range (R80) /mm			
	DECT	SECT	
Head	(a)	0.00	-1.40
	(b)	1.00	-0.20
	(c)	1.30	0.50
	(d)	0.50	-1.40
	(e)	2.20	0.80
	(f)	-4.70	-8.10
	(g)	1.90	0.10
	(h)	2.20	1.00
	(i)	2.80	0.80
	(j)	-4.90	-8.90
	(k)	2.60	0.6
(l)	2.90	0.4	
Mean error	0.65	-1.32	
RMS error	2.67	3.56	
Spread	7.80	9.90	
Shin	(a)	1.00	0.20
	(b)	0.50	-0.40
	(c)	0.80	-0.60
	(d)	1.40	0.20
	(e)	0.90	-0.40
	(f)	1.50	-0.30
Mean error	1.02	-0.22	
RMS error	1.07	0.38	
Spread	1.00	0.80	

All measurements across both samples		
Mean error	0.77	-0.95
RMS error	2.26	2.91



# WP2: Conclusions

- DECT predicts range with an overall accuracy comparable to the SECT technique currently in use.
- Existing SECT technique is very accurate!
- DECT not consistently superior for all tissue types with this experimental setup.
- The work provided a valuable end-to-end test of the methodology and demonstrated the feasibility of the technique.

# WP3: Sensitivity analysis of an empirical method of DECT implementation

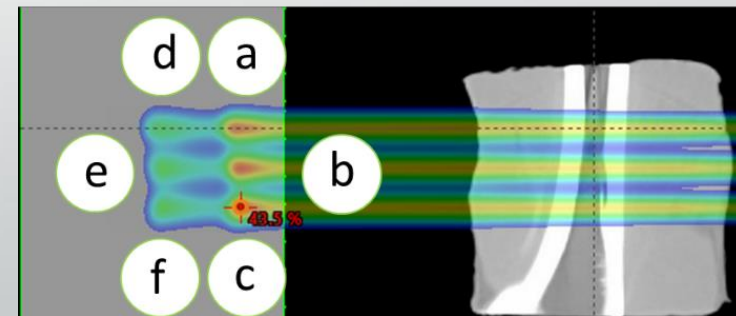
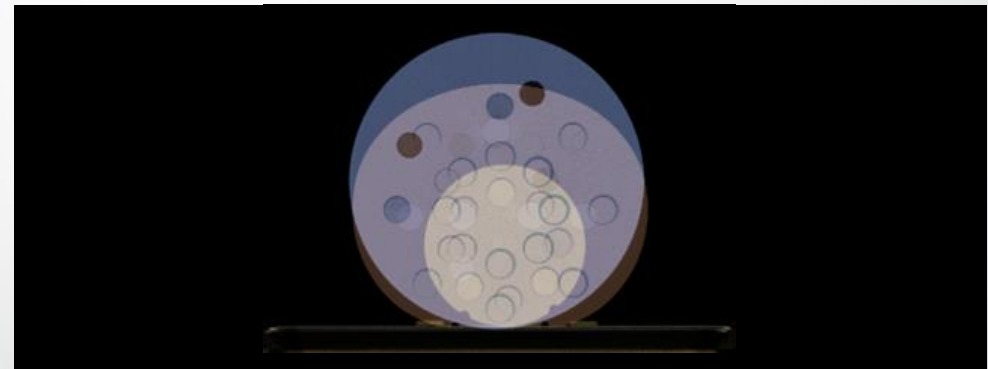
- This work represents extended analysis of the empirical method in the clinical setting.
- It draws on other uncertainty themes from the literature and brings it all together in one analysis which is representative of the rigorous approach applied to any new clinical technique.
- Analysis includes sensitivity of predicted SPR to:
  - Choice of calibration phantom
  - CT scan parameters
  - Reference tissues used for biological optimisation
  - Imaging noise
  - Movement between dual-spiral scans

# WP3: Methods

The same tissue surrogate inserts were used in **3 different phantom sizes**.



Different SPR maps were generated for the animal tissue sample scans based on each calibration.





# WP3: Methods

DECT calibration was also repeated with **iBHC** both on and off for the animal tissue scans.

**Different tissue sets** were used for the biological optimisation and the cut-off point between bone and soft tissue was also varied by +/-100 HU to investigate the impact of tissue classification.

DECT scans were repeated with reduced mAs to **increase the noise** in the image.

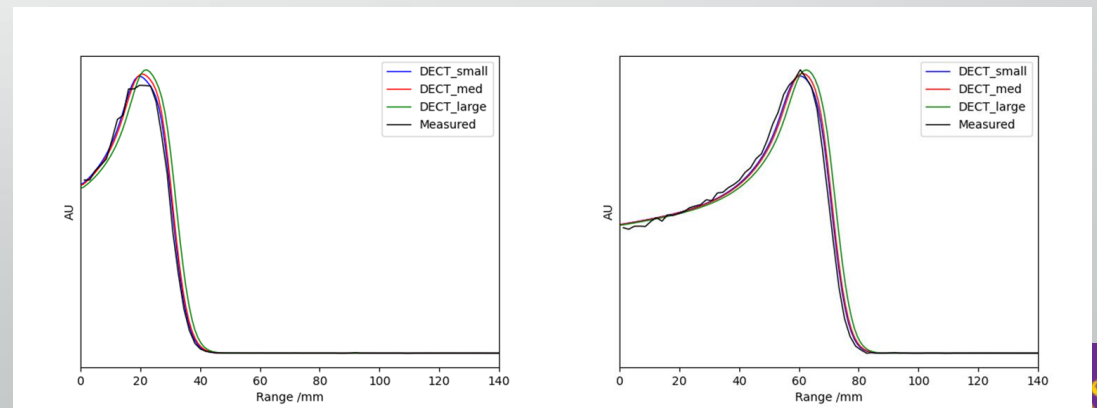
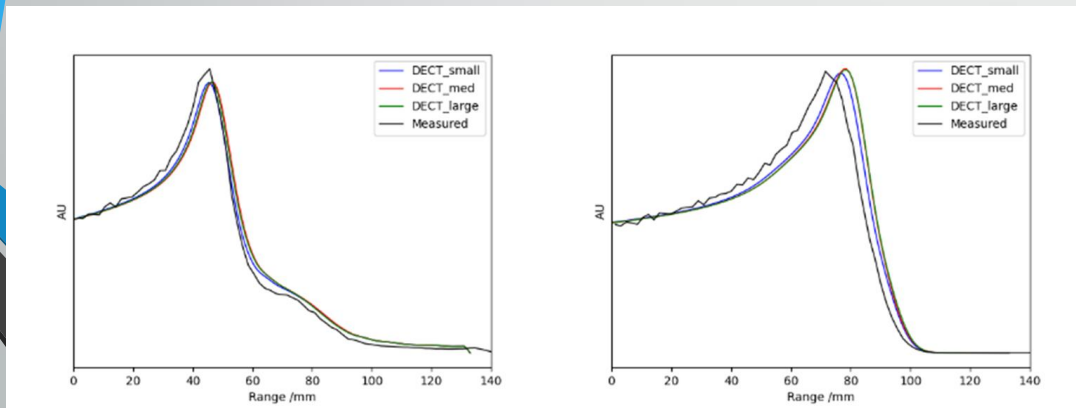
	mAs used for pig head scans		mAs used for cow shin scans	
	80 kVp	140 kVp	80 kVp	140 kVp
Clinical CT protocol	310	75	289	66
CT protocol with increased imaging noise	157	37	137	33

The ICRP computational phantom was used and a **shift** applied to one of the images to simulate the movement of a patient between the scans.

# WP3: Results - phantom

	Residual range errors in Pig head sample		Residual range errors in Cow shin sample	
	Mean /mm	RMS /mm	Mean /mm	RMS /mm
Small phantom (small CIRS)	0.65	2.67	1.02	1.07
Medium phantom (complete CIRS)	1.41	3.29	1.48	1.54
Large phantom (Gammex)	1.46	3.09	2.48	2.52

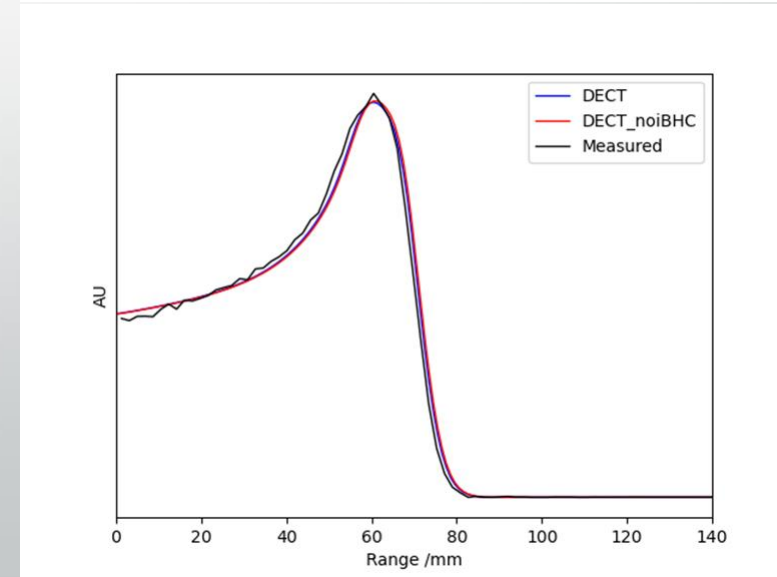
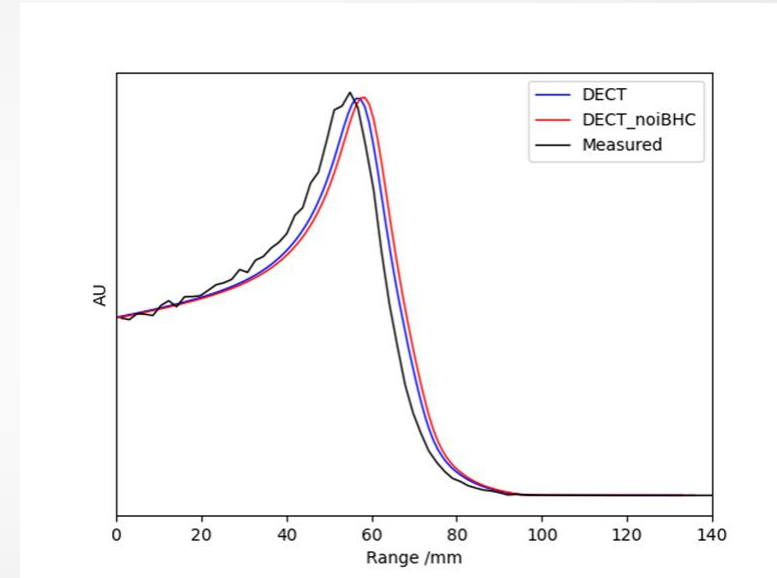
In general, the range predicted by the small DECT calibration gives the closest match to measurement.



# WP3: Results - iBHC

Removing the iBHC from the DECT reconstruction changes the effective energy of the scan. The impact on the predicted residual range is greater in the (larger) head sample than the shin sample.

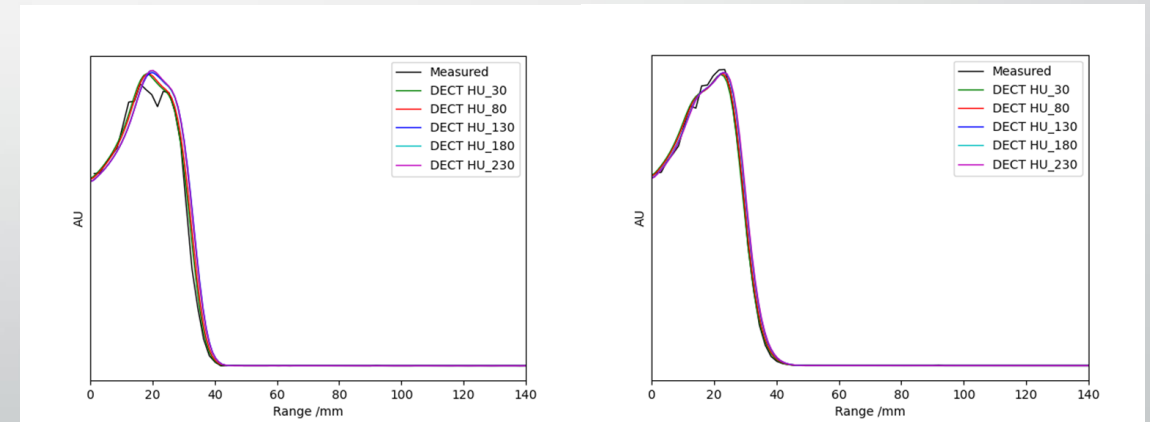
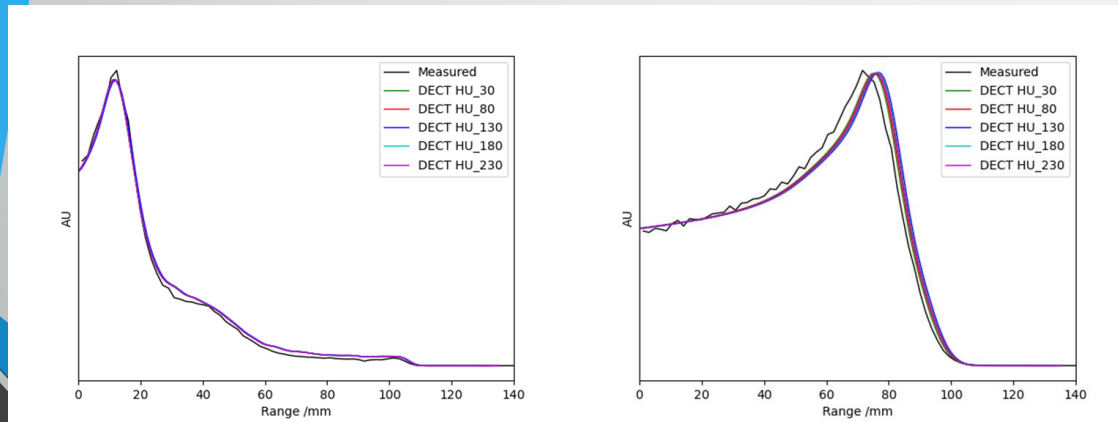
	Original DECT methodology (with iBHC)		DECT without iBHC applied	
	80 kVp (low)	140 kVp (high)	80 kVp (low)	140 kVp (high)
$E_{eff}$ (keV)	60	81	62	84
$A^{soft}$	994.1	994.3	992.8	993.2
$B^{soft}$	0.997	0.996	0.996	0.996
$A^{bone}$	1003.5	994.9	1029.4	1023.6
$B^{bone}$	0.994	0.988	0.951	0.968



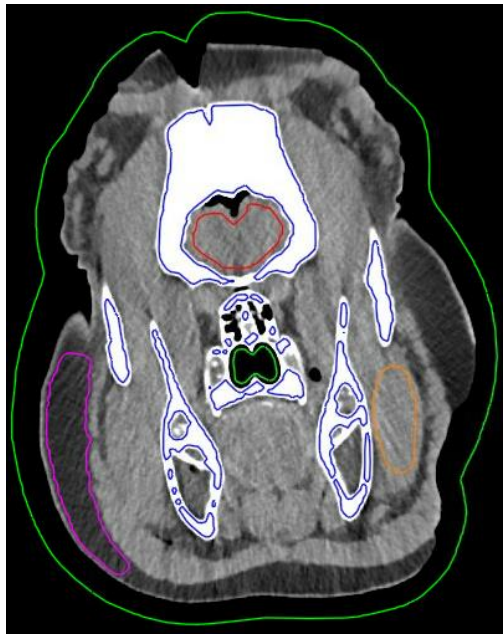
# WP3: Results – reference tissues

The DECT method is insensitive to the choice of reference tissue set based on the results of this analysis

	Calibration: ICRP tissues (ICRP, 2009)		Calibration: White et al. (ICRU, 1989; White et al., 1987)	
	ICRP (SPR)	White et al. (SPR)	ICRP (SPR)	White et al. (SPR)
RMS error % (all tissues)	0.51	0.66	0.48	0.63
RMS error % (bone tissues)	0.63	0.61	0.57	0.54
RMS error % (soft tissues)	0.40	0.68	0.40	0.67
RMS error % (soft tissues excluding lung)	0.26	0.31	0.42	0.40



# WP3: Results – imaging noise

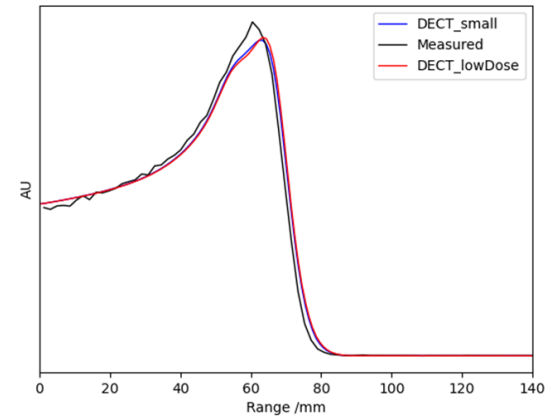
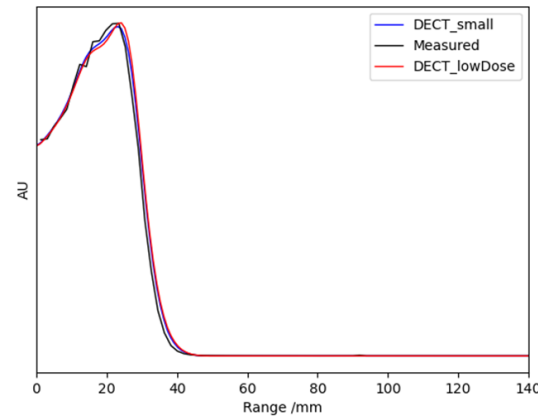
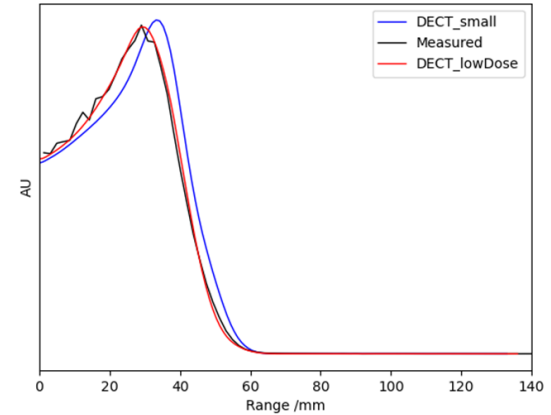
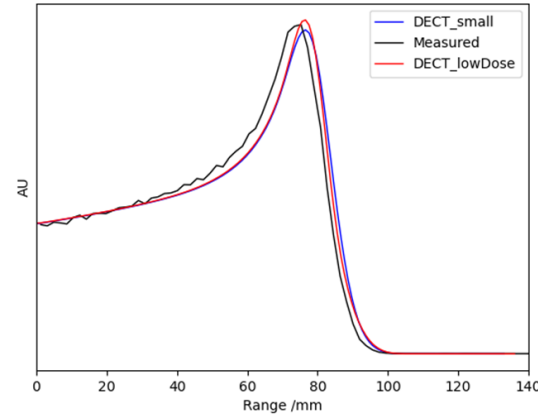


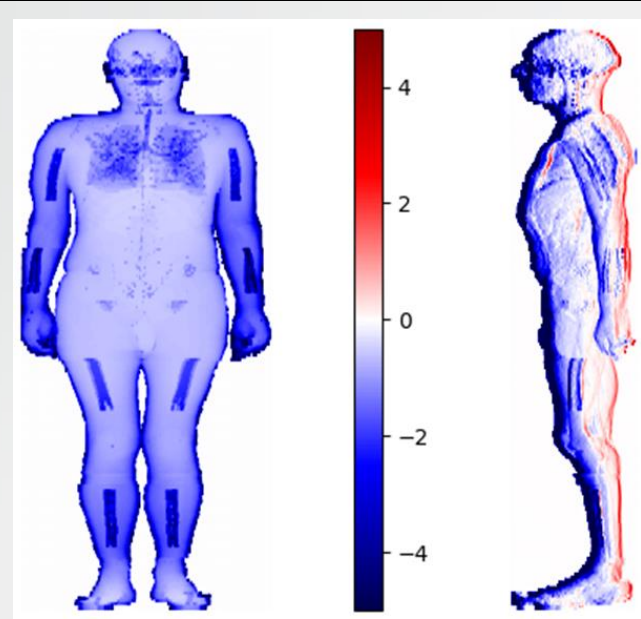
80 kVp scan 310 mAs



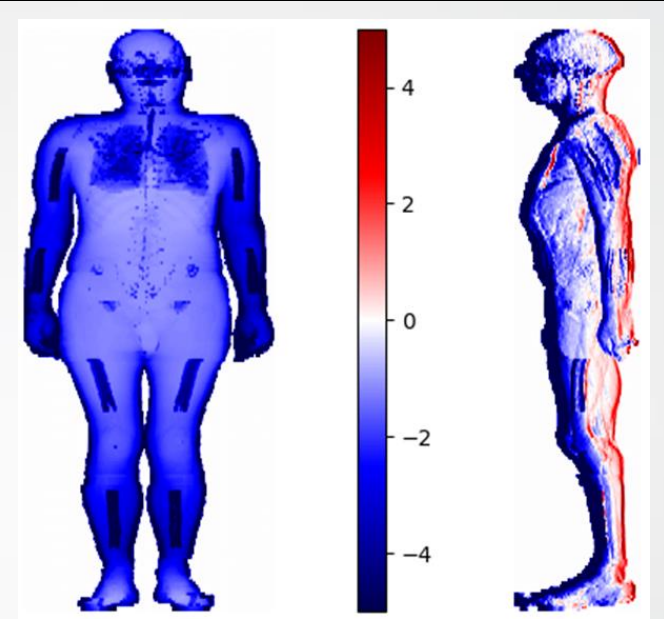
80 kVp scan 157 mAs

Mean HU	SD HU	SNR	Tissue ROI	Mean HU	SD HU	SNR
963.6	315.3	3.06	Bone (blue)	957.5	314.4	3.05
-56.7	12.13	4.67	Adipose (pink)	-60.5	15.26	3.96
55.4	20.0	2.77	Brain (red)	55.0	22.58	2.43
63.1	12.1	5.21	Soft tissue (orange)	63.8	14.5	4.4
-950.3	110.76	8.58	Air cavity (green)	-951.0	113.7	8.36

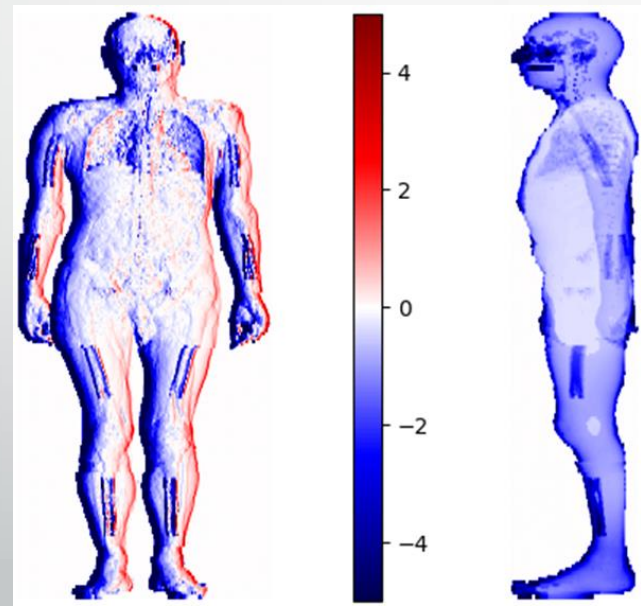




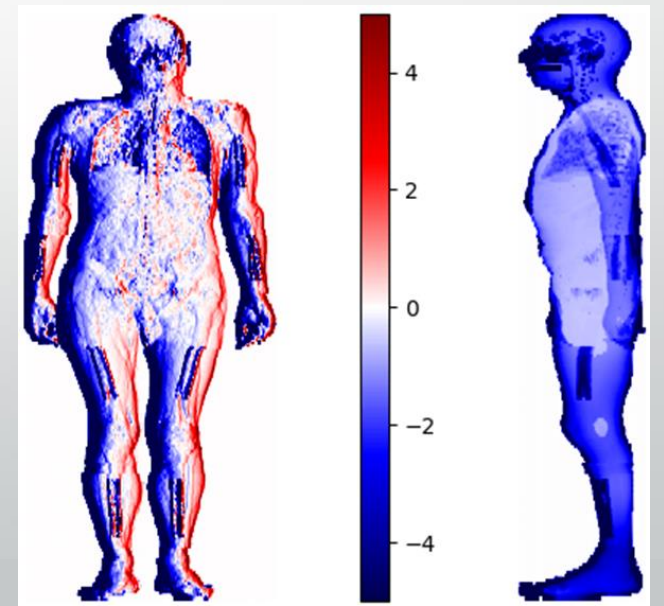
(a) Shift of 0.7 mm in A-P direction



(b) Shift of 1.4 mm in A-P direction



(c) Shift of 0.7 mm in R-L direction



(d) Shift of 1.4 mm in R-L direction

# WP<sub>3</sub>: Results - movement

# WP3: Conclusions

- Those factors which affect the HU values reported by the scanner have an impact on the accuracy of predicted SPR.
  - Calibration phantom size
  - Beam hardening correction
  - Imaging noise
- The effective use of iBHC and the optimisation of DECT SPR prediction to account for phantom size would be enough to guarantee safe and effective PBT delivery.
- The most significant sensitivity in the method is the presence of movement between the two CT scans. This sensitivity limits the potential implementation of this method to those sites where motion is of no concern e.g. BoS / CNS.

# Further work

- Additional experimental measurements to try and isolate some of the sources of error.
- Pilot study on BoS patients to determine if there is a material advantage when using DECT in PBT treatment planning.
- If pilot successful, commission technique as an option (with the additional calibration methods) that a consultant could request if desired.
- If sites beyond BoS are investigated then additional calibrations for patient size will be required.
- Collaboration with UCLH



# Conclusions

- Demonstrated that implementation of an empirical DECT methodology is feasible and practical.
- Added value to the original publications of this method through further theoretical and experimental validation and sensitivity analysis.
- Provided insight into those factors which are important to consider for any clinical implementation of DECT.

# References

- Goitein, M. (1977). *The measurement of tissue heterodensity to guide charged particle radiotherapy. International Journal of Radiation Oncology, Biology, Physics*, 3(C), pp.27–33.
- Han, D., Siebers, J. V. and Williamson, J.F. (2016). *A linear, separable two-parameter model for dual energy CT imaging of proton stopping power computation. Medical Physics*, 43(1), pp.600–612.
- Hünemohr, N. et al. (2013). *Ion range estimation by using dual energy computed tomography. Zeitschrift für Medizinische Physik*, 23(4), pp.300–313. [online]. Available from: <http://dx.doi.org/10.1016/j.zemedi.2013.03.001>.
- Lalonde, A. and Bouchard, H. (2016). *A general method to derive tissue parameters for Monte Carlo dose calculation with multi-energy CT. Physics in Medicine and Biology*, 61(22), pp.8044–8069.
- Landry, G. et al. (2013). *Deriving effective atomic numbers from DECT based on a parameterization of the ratio of high and low linear attenuation coefficients. Physics in Medicine and Biology*, 58(19), pp.6851–6866.
- Schneider, U., Pedroni, E. and Lomax, A. (1996). *The calibration of CT Hounsfield units for radiotherapy treatment planning. Phys. Med. Biol.*, 41, pp.111–124.
- Taasti, V.T., Petersen, J.B.B., et al. (2016). *A robust empirical parametrization of proton stopping power using dual energy CT. Medical Physics*, 43(10), pp.5547–5560.
- Wohlfahrt, P., Möhler, C., Stützer, K., et al. (2017). *Dual-energy CT based proton range prediction in head and pelvic tumor patients. Radiotherapy and Oncology*, 125(3), pp.526–533.
- Yang, M et al. (2010). *Theoretical variance analysis of single- and dual-energy computed tomography methods for calculating proton stopping power ratios of biological tissues. Physics in Medicine and Biology*, 55, pp.1343–1362.



# Additional slides

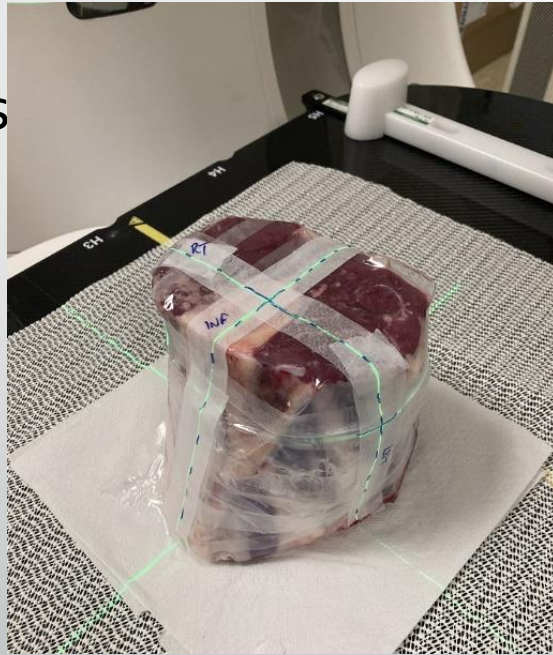
# Literature review

Several methods of predicting SPR using DECT are outlined in the literature

- **Parameterisation methods** rely on the determination of properties such as electron density ( $\rho_e$ ), effective atomic number ( $Z_{eff}$ ) and mean excitation energy ( $I$ ) to be used with Bethe equation to determine SPR.
- **Basis Vector Model** assumes that the attenuation coefficient ( $\mu$ ) of a material can be represented as a linear combination of  $\mu$  for 2 basis materials. Use the  $\rho_e / Z_{eff} / I$  of these basis materials to predict the same parameters for a voxel containing an unknown material.
- **Tissue decomposition** uses a representation of human tissues based on a principal component analysis. Eliminates the intermediate step of determining tissue parameters.
- **Empirical method** uses empirical equations developed to predict SPR based on DECT images only with no intermediate parameter calculations.

# WP2: Methods

- Animal tissue scanned at 120 kVp (with 100% filtration) and at 80 / 140 kVp (with 100% filtration)



(a) Cow shin mark-up and positioning for CT scan

at 120 kVp (with 100% filtration)



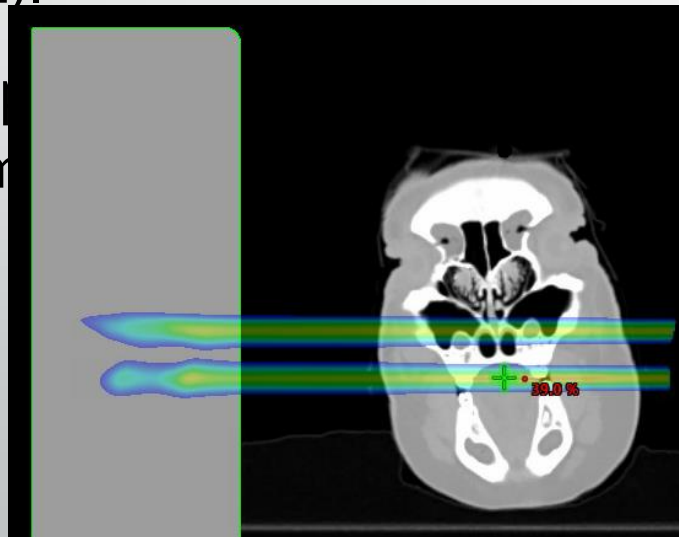
(b) Pig head positioned in vacuum bag for CT scan

and at 80 / 140 kVp (with 100% filtration)

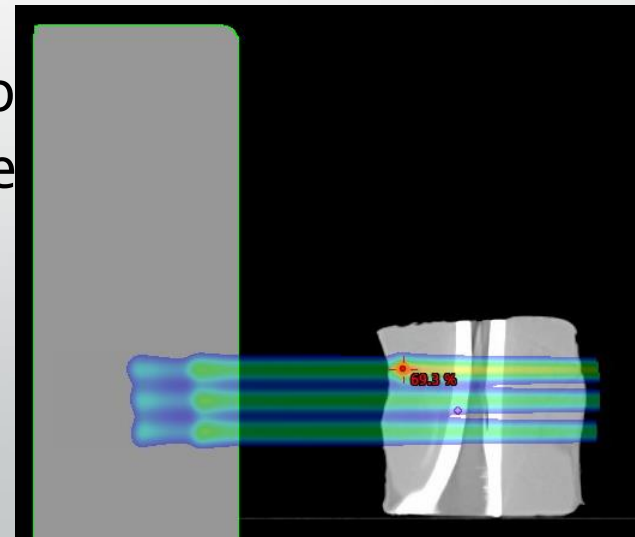
# WP2: Methods

- An SPR map was created from the DECT scans using the python code written as part of WP1.
- SPR map imported to Eclipse with a specific DECT calibration curve (1000:1).

- A spot p  
the sam



(a) Spot transmission through pig head



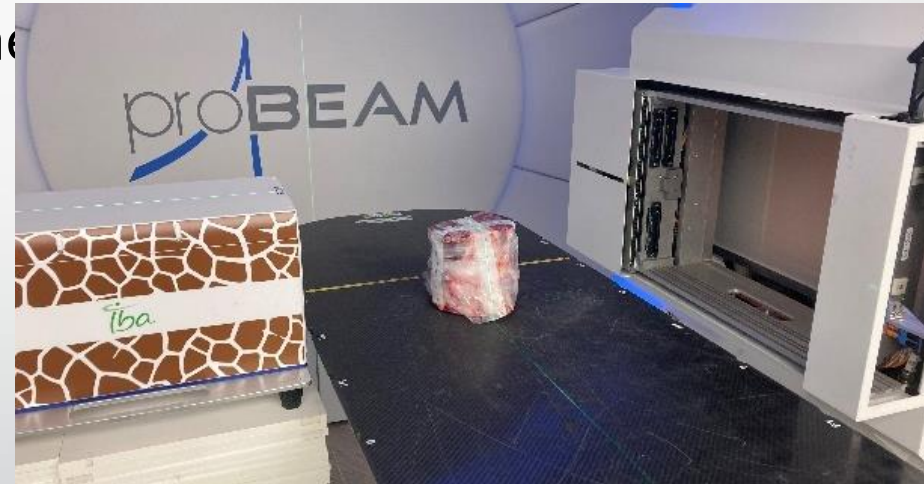
(b) Spot transmission through cow shin

pass through

# WP2: Methods

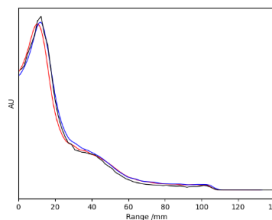


(a) Range measurement setup for pig head

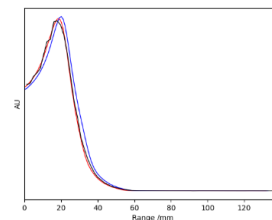


(b) Range measurement setup for cow shin

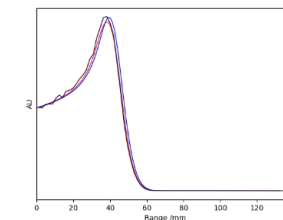
# WP2: Re



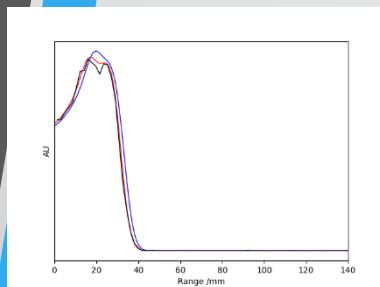
(a) 120MeV



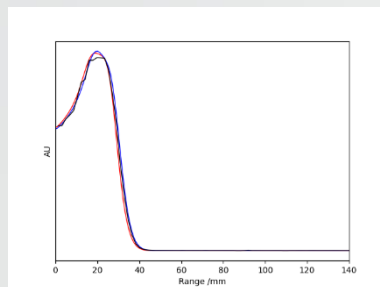
(b) 140MeV



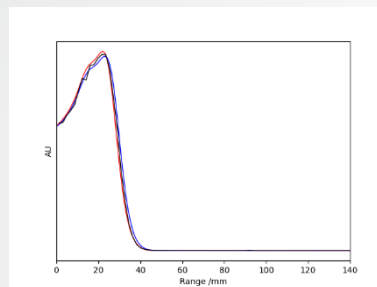
(c) 140MeV



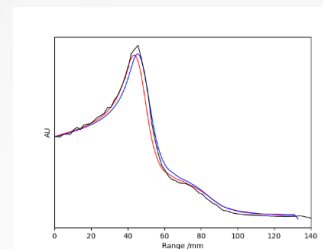
(a) 160MeV



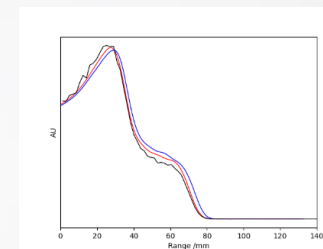
(b) 160MeV



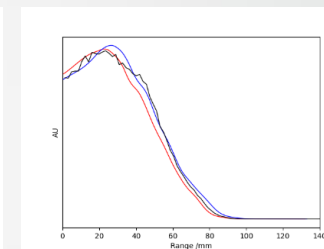
(c) 160MeV



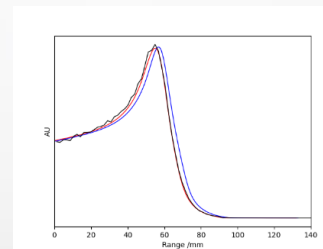
(d) 140MeV



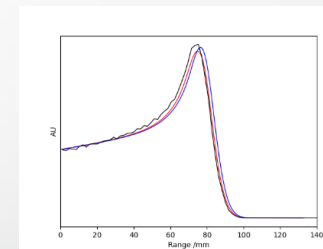
(e) 160MeV



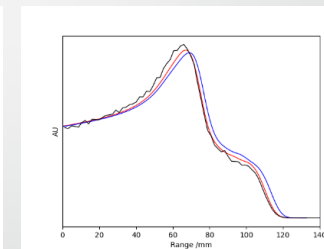
(f) 160MeV



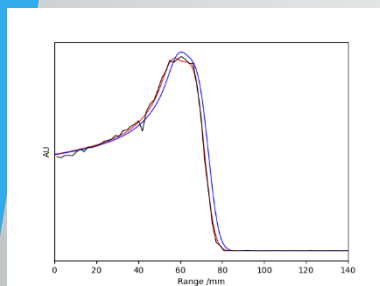
(g) 160MeV



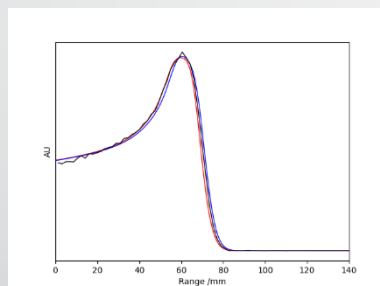
(h) 160MeV



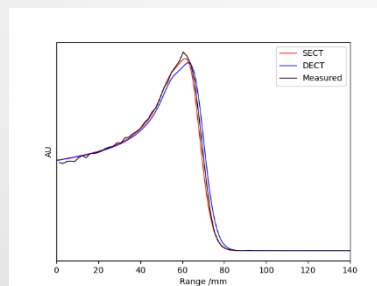
(i) 180MeV



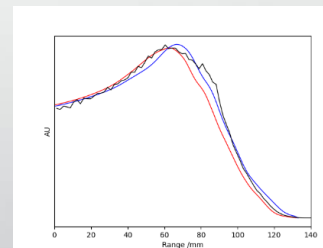
(d) 180MeV



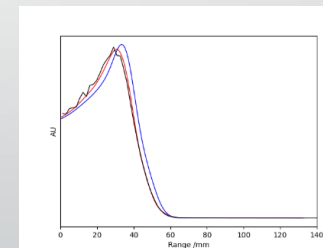
(e) 180MeV



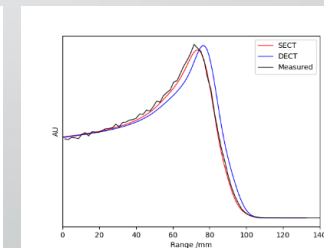
(f) 180MeV



(j) 180MeV



(k) 180MeV



(l) 200MeV

